**THE COMPOSITIONAL AND PHYSICAL PROPERTIES OF LOCALIZED PYROCLASTIC DEPOSITS.**

D. Trang[1], J. J. Gillis-Davis[1], M. Lemelin[1], J. T. S. Cahill[2], R. R. Ghent[3,4], B. R. Hawke[1], and T. A. Giguere[1], [1]University of Hawai'i at Mānoa, Hawai'i Institute of Geophysics and Planetology, Honolulu, HI (dtrang@higp.hawaii.edu), [2]Applied Physics Laboratory, Johns Hopkins University, Laurel, MD, [3]Department of Earth Sciences, University of Toronto, Toronto, ON, [4]Planetary Science Institute, Tucson, AZ

**Introduction:** There are more than fifty localized pyroclastic deposits on the lunar surface [1]. Localized pyroclastic deposits are small deposits (<2500 km$^2$) that exhibit a low albedo and a smooth surface [2]. These deposits exist within floor-fractured craters and the margins of major mare regions. Furthermore, these deposits commonly occur in isolation instead of overlapping deposits. The center of these deposits typically displays an irregular-shaped crater, which is thought to be the volcanic vent.

Previous work has explored the eruptive properties of localized pyroclastic deposits [i.e., 1–4]. In investigating six localized pyroclastic deposits in the Alphonsus region, [3] explored the volume and fractions of juvenile and non-juvenile material and the shape of the deposits and vents. They tested several eruption models to match their observations. They found that localized pyroclastic deposits are likely to be products of vulcanian-style eruptions. They suggested that magma intruded into the crust as a dike, which stalled at hydrostatic elevations and cooled into a basaltic cap. Then, volatiles begin to accumulate beneath the basaltic cap causing a build up in pressure until decompression and a transient eruption.

Later, *Hawke et al.* [4] built upon *Head and Wilson's* [3] work by investigating the compositional variation among localized pyroclastic deposits across the lunar nearside. They noticed three types of localized pyroclastic deposits: Class I deposits exhibit both glass and highlands material, Class II deposits show glass and mare material, and Class III deposits show glass and olivine. They suggested that Class I and II entrained local material and glass. Class III originated from glass and olivine-bearing magma or devitrification of pyroclastic glass into olivine.

**Methods:** We studied the compositional and physical properties of 34 previously identified localized pyroclastic deposits [i.e., 1, 5]. To examine the compositional nature of these deposits, we used radiative transfer techniques with the Multispectral Imager, a Kaguya instrument [6], at 62 m/pixel to determine the crystalline to glass proportions [7]. The radiative transfer techniques are based upon the equations of [8] and [9] adjusted the technique to become applicable to lunar spectral data. As a result, we produced olivine, orthopyroxene, clinopyroxene, plagioclase, and glass abundance maps for these deposits. For each mineral map, we computed the mean proportions from the pixels in each deposit.

To investigate the physical properties, we examined the 12.6-cm (S-band) Mini-RF circular polarization ratio (CPR) map at 100 m/pixel and the surface rock abundance map, which was derived from Diviner data, at 128 m/pixel. The CPR map shows rocks that are >1 cm in size on the surface and subsurface [10, 11]. In contrast, the surface rock abundance map displays rocks >1 m and only on the surface [12]. We calculated the mean CPR and surface rock abundance from the pixels within each deposit.

We also calculated the maximum thickness of each localized pyroclastic deposit from the Wide Angle Camera (WAC) digital terrain model (DTM). To determine the maximum deposit thickness, we needed to model the pre-erupted surface. First, we deleted DTM pixels within the pyroclastic deposit. Next, we used a script in ArcGIS called "spline with barriers", which used pixels outside the deposit to interpolate within the deposit; thus, this interpolation formed the pre-erupted DTM. Finally, we subtracted each pixel in the pre-erupted DTM from the original DTM. To extract the maximum deposit thickness, we searched for the pixel that has the largest difference between the DTM and the pre-erupted DTM. This method is similar to the work by [3].

**Results:** We found that there is a relationship between the glass proportion, surface rock abundance, and the maximum pyroclastic deposit thickness (Fig. 1). We observed that crystalline-rich deposits (<60 vol.% glass) exhibit thicknesses to about ≲50 m (Fig. 1a). On the other hand, glass-rich deposits (≥60 vol.% glass) with increasing glass proportions also display increasing maximum deposit thickness. When examining surface rock abundance relative to glass proportions (Fig. 1b), we noticed two distinct clusters, one cluster with high proportion of glass (≳40 vol.%) and low surface rock abundance (≲0.36%) and another cluster with low glass proportion (around ≲40 vol.%) with high surface rock abundance (around ≳0.36%). Additionally, we observed two minor clusters as well, one with low rock abundance (≲0.36%) and high degree of crystallinity (≲60 vol.%) glass. The other minor cluster contains high surface rock abundance (≳0.36%) and high glass proportions (≳60 vol.%).

**Discussion:** After we examined the surface glass proportions, surface rock abundances, and maximum deposit thickness relative to one another, we classified the clusters into four groups: the Glassy, Crystalline, Blocky, and Hybrid. In contrast to other groups, Glassy pyroclastic deposits have high glass proportions, tend to have thicker deposits, and low CPR and surface rock abundances. The Blocky pyroclastic group is similar to the Glassy group except these deposits exhibit greater surface rock abundance and higher CPR. The Crystalline group on the other hand displays thin deposits and low glass proportions than the Glassy Group. As for the Hybrid group, these deposits show thin deposits, low to non-existent glass proportions and high surface rock abundance and CPR, which are similar to the surrounding area.

We used *Head and Wilson's* [3] eruption model to derive an interpretation of the origin of each pyroclastic deposit group. First, the Glass group is different from the Blocky group because the Blocky group has greater surface rock abundance and CPR. We interpreted that these two groups eruptive histories are similar with the exception that the Blocky group erupted larger fragments than the Glassy group. Between the Glassy and Crystalline group, they contrast from each other in glass proportions and deposit thicknesses. We suggested that the Crystalline pyroclastic deposit group are short-lived volcanoes that erupted mostly the basaltic cap with some glass. On the other hand, the Glassy pyroclastic deposits are long-lived volcanoes that initially erupted the basaltic cap in the beginning of their lives and evolved to eject more glass later. As for the Hybrid group, their properties are similar to mare basalt, which we suggested that these deposits may have been pyroclastic eruptions at one point, but later transitioned to effusive volcanism that partially or completely buried these deposits.

**Conclusion:** We characterized the surface rock abundance, CPR, maximum deposit thickness, and mineral proportions of localized pyroclastic deposits. From investigations into the physical and compositional properties of localized pyroclastic deposits, we found that the deposits can be divided into four groups, Glassy, Blocky, Crystalline, and Hybrid.

**Future Work:** There are at least two more additions to improve this work. First, we will include cluster analysis to verify the presence of our four groups. Second, we will verify our interpretations of each group through eruption models similar to the work by *Head and Wilson* [3].

**References:** [1] Gaddis L. R. et al. (2003), *Icarus*, *161*, 262–280. [2] Gaddis L. R. et al. (2000), *JGR*, *117*, 4245–4262. [3] Head J. W. and Wilson L. (1979), *Proc. Lunar Sci. Conf. 10th*, 10, 2861–2897. [4] Hawke B. R. et al. (1989), *Proc. Planet. Lunar Sci. Conf. 19th*, 19, 255–268. [5] Gustafson, J. O. et al. (2012), *JGR*, *117*, E00H25. [6] Ohtake M. et al. (2008), *Earth Planets Space*, *60*, 257–264. [7] Lemelin, M. (*submitted*), *JGR*. [8] Hapke, B. (1993) *Theory of Reflectance and Emittance Spectroscopy*, 469. [9] Lucey, P. G. (2014), *Am. Mineral*, *99*, 2251–2257. [10] Carter, L. M. (2011), *Proc. of the IEEE*, *99(5)*, 770–782. [11] Ghent, R. R. (2005), *JGR*, *110*, E02005. [12] Bandfield J. L. et al. (2011), *JGR*, *116*, E00H02. [13] Cahill J. T. S. (2014), *Icarus*, *243*, 173–190.

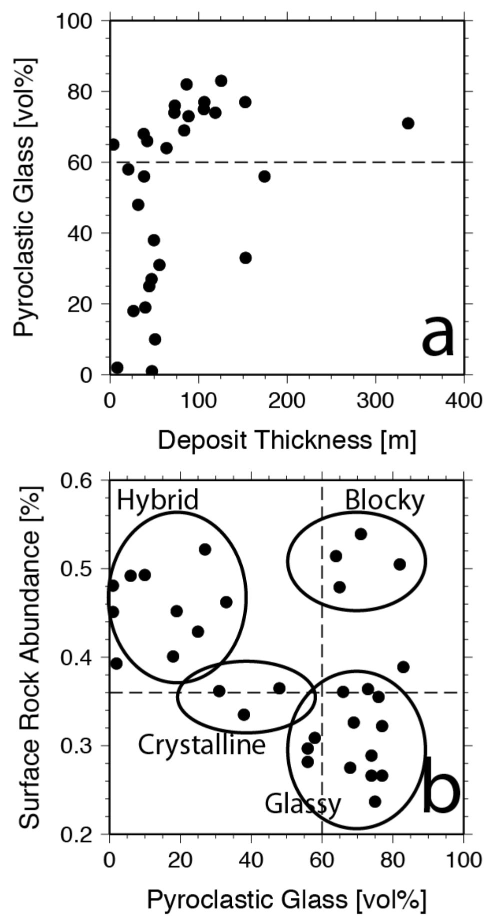


**Figure 1**: (a) Comparison between maximum deposit thickness and pyroclastic glass proportions. The dotted line separates from constant thickness to a gradual increase in deposit thickness with increasing glass proportions. (b) Comparison between glass proportion and surface rock abundance. The horizontal line is where the surface rock abundance is 0.36%, an approximation of the minimum surface rock abundance of the maria [13]. The vertical line is at 60 vol.% glass, which is related to where the deposit thickness begin to gradually increase with increasing glass proportions.